

## Anode Properties of Composite Thick-Film Electrodes Consisted of Si and Various Metal Silicides

Hiroyuki Usui, Kazuki Meabara, Koji Nakai, and Hiroki Sakaguchi\*

Department of Chemistry and Biotechnology, Graduate School of Engineering, Tottori University  
4-101 Minami, Koyama-cho, Tottori 680-8552, Japan

\*E-mail: [sakaguch@chem.tottori-u.ac.jp](mailto:sakaguch@chem.tottori-u.ac.jp)

Received: 6 April 2011 / Accepted: 18 April 2011 / Published: 1 June 2011

---

Thick-film electrodes of composite active materials consisted of Si and various metal silicides, FeSi<sub>2</sub>/Si, VSi<sub>2</sub>/Si, or MmSi<sub>2</sub>/Si, were prepared by mechanical alloying followed by gas deposition for anodes of Li-ion batteries. We investigated a relationship between the performance of these electrodes and properties of the silicide, the electrical resistivity, the referential breaking strength, and the thermodynamic stability. The MmSi<sub>2</sub>/Si composite electrode exhibited superb cycling performance, where the discharge capacity of 380 mA h g<sup>-1</sup> was maintained even at the 1000th cycle. It is suggested that thermodynamically stable MmSi<sub>2</sub> in the composite electrode can improve the electrical conductivity of the electrode and can release the stress induced by a volumetric change of Si for a long period.

---

**Keywords:** Si anode, composite active material, metal silicide, gas deposition, Li-ion battery

### 1. INTRODUCTION

Silicon has a huge theoretical capacity of about 4200 mA h g<sup>-1</sup>, which makes it an attractive anode material in Li-ion batteries. The huge capacity is originated from an alloying reaction of Li-Si up to a composition of Li<sub>4.4</sub>Si [1-3]. However, Si anode has some disadvantages of a high electrical resistivity, a low diffusion coefficient of Li ion in Si [4], and a drastic change of specific volume during the alloying/dealloying reactions [5,6]. The volume per Si atom in cubic Li<sub>22</sub>Si<sub>5</sub> (Li<sub>4.4</sub>Si) structure is 0.0824 nm<sup>3</sup> [7], which is approximately 410% larger than that of 0.020 nm<sup>3</sup> in the original Si structure. This drastic change in volume generates an immense stress as high as 1 GPa [8] in the Si anode. Such high pressure easily causes a breakup of the electrode and an electrical isolation of the active material of Si, resulting in increased irreversible capacity and reduced electrochemical performance in earlier charge-discharge cycles. When a silicide is used instead of elemental Si as the

active material of the anode, the discharge capacity is drastically degraded, owing to the smaller storage amount of Li ions in the silicide. Therefore, we believe that anodes for next-generation Li-ion batteries should mainly consist of elemental Si to take an advantage of its huge theoretical capacity.

Gas deposition (GD) is a very favorable technique to prepare thick films. An aerosol consisting of a high-pressure carrier gas and active material particles is jetted near the speed of sound from a nozzle onto a substrate. As a technique forming thick-film anodes, the gas-deposition method has some attractive advantages including (i) the strong adhesion between the active material particles as well as between the particles and the substrate, (ii) the nearly unchanging composition in the thick film formed without atomization (*e.g.*, vaporization) of the particles, and (iii) the formation of interstitial spaces between particles, which is a favorable structure to release the stress induced by the volumetric change of the active material particles [9].

Various binary silicides,  $\text{Mg}_2\text{Si}$  [10],  $\text{CaSi}_2$  [11,12],  $\text{CoSi}_2$  [11,13],  $\text{NiSi}_2$  [11,14], and  $\text{TiSi}_2$  [15], have been already studied as anode materials of Li-ion battery. In these silicides,  $\text{Mg}_2\text{Si}$  and  $\text{CaSi}_2$  exhibited larger reversible capacity at the first cycles because alkaline-earth elements, Mg and Ca, are active metals to Li. However, during the first lithiation of  $\text{Mg}_2\text{Si}$  or  $\text{CaSi}_2$ , their crystal structures collapsed to form binary alloys of Li–Mg or Li–Ca in addition to Li–Si, resulting in poor cycling performance of these electrodes. On the other hand, Co, Ni, and Ti are inactive metals to Li. Electrodes of  $\text{CoSi}_2$ ,  $\text{NiSi}_2$ , and  $\text{TiSi}_2$ , showed reversible capacities limited to less than  $200 \text{ mA h g}^{-1}$  [11]. However, good cycleability is expected for the electrodes because these silicides do not form binary alloys of Li and these transition metals during the lithiation. We have prepared composite thick-film electrodes of Si-based materials combined with silicides or germanides, and have demonstrated that the electrode performance is significantly improved by the synergetic effects of the properties of Si and the combined materials [16–20]. One of these electrodes, using a composite active material consisting of lanthanum silicide ( $\text{LaSi}_2$ ) and Si with weight ratio of 70:30, has exhibited remarkably improved electrode performance [17]. As a reason of the improvement, it is suggested that  $\text{LaSi}_2$  phase surrounds Si phase in individual composite particles, and that the  $\text{LaSi}_2$  matrix in the composite electrode releases the stress generated in Si particles during the lithiation and considerably improves low electrical conductivity of the composite electrode.

In this study, we used various metal silicides,  $\text{FeSi}_2$ ,  $\text{VSi}_2$ , and mischmetal silicide ( $\text{MmSi}_2$ ) for matrix materials in the composite thick-film electrodes, and investigated their anode properties comparing with the property of the  $\text{LaSi}_2/\text{Si}$  composite electrode. In particular, we studied the reason of the improved performance from the viewpoint of the silicides' mechanical, electrical, and thermodynamic properties.

## 2. EXPERIMENTAL

Active material powder of composite metal silicides,  $\text{MSi}_2/\text{Si}$  ( $M = \text{Fe}, \text{V}, \text{and Mm}$ ), was synthesized by a mechanical alloying (MA) method. Chips of metals (Fe, V, and Mm) and Si powder were mixed so that the weight ratio of  $\text{MSi}_2:\text{Si}$  is 70:30. Due to the excess Si, composite active materials consisting of Si and metal silicides are expected to be synthesized. Mischmetal used in this

study contains 22% of La, 60% of Ce, 4% of Pr, and 14% of Nd in weight ratio. The mixture was put in a zirconia pot together with zirconia balls. The weight ratio of the balls to the mixture was set to be 15. The pots were sealed with an O-ring to keep an atmosphere of dry Ar gas. The MA was performed using a high-energy planetary ball mill at 300 rpm and at room temperature, and was continued for 5–50 hours until alloyed powder exhibited X-ray diffraction (XRD) peaks of each metal silicide,  $\text{FeSi}_2$  (JCPDS No.35-0822),  $\text{VSi}_2$  (JCPDS No.38-1419), and  $\text{MmSi}_2$ . The milling time for  $\text{FeSi}_2$  and  $\text{VSi}_2$  was set to be 50 and 30 hours. For  $\text{MmSi}_2$  and  $\text{LaSi}_2$ , the milling time was 5 hours. The peaks of  $\text{MmSi}_2$  were indexed as those of  $\text{LaSi}_2$  (JCPDS No.06-0471). The XRD patterns were obtained for the silicide samples covered with polyimide films in Ar gas to avoid oxidation of the silicides. In addition, a composite active material consisting of Si and metal silicides ( $\text{FeSi}_2$ ,  $\text{VSi}_2$ , and  $\text{MmSi}_2$ ) was also synthesized by MA under the same conditions.

The crystal structure of the composite silicide powder was studied by using an X-ray diffractometer (XRD-6000 Shimadzu Co., Ltd.). A reference breaking strength of the active material powder was measured by a uniaxial compression test using a dynamic ultra-micro hardness tester (DUH-211S, Shimadzu Co. Ltd.). In this study, the reference breaking strength was defined as an applied pressure when a compressed particle of the powder showed 10% deformation compared with its original size. The electrical resistivity was measured for pristine Si powder and the composite metal silicide powders under a uniaxial press of 55 MPa using a two probes method in Ar atmosphere.

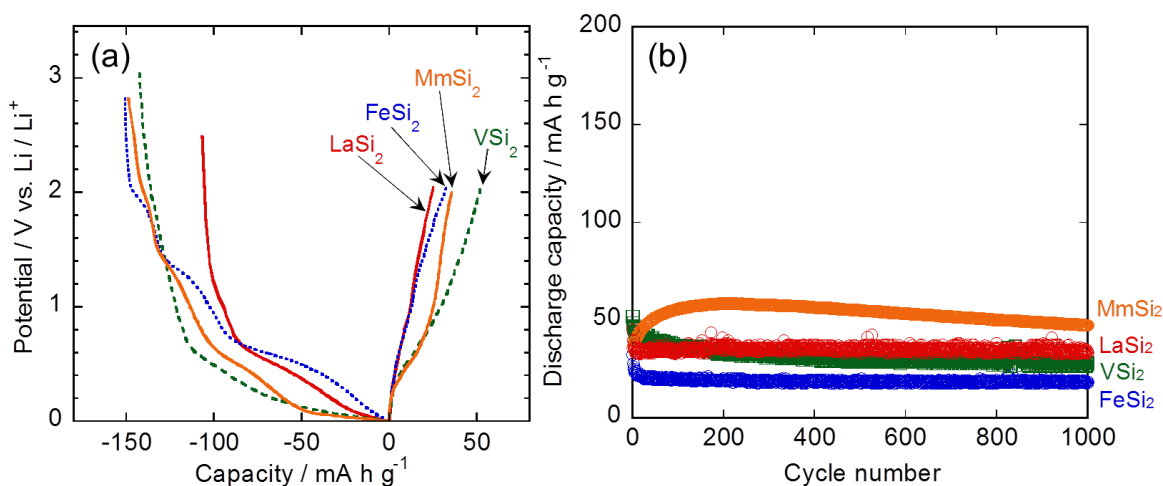
For gas deposition [16-21], Cu foil substrates with 20  $\mu\text{m}$  in thickness were set up in a vacuum chamber with a guide tube. An aerosol consisting of Ar gas (differential pressure:  $7 \times 10^5$  Pa) and active material powders was generated in the guide tube, and sprayed from a nozzle onto the Cu substrate in the chamber with a base pressure of approximately 20 Pa. The nozzle diameter and the distance from nozzle to substrate were set to be 0.8 mm and 10 mm, respectively. The thickness of the obtained thick-films on the substrates was not uniform, but was estimated to basically range from 2 to 5  $\mu\text{m}$  by observing the cross section of the films by scanning electron microscopy (SEM, JSM-5200, JEOL Ltd.).

Electrochemical measurements were carried out with a beaker-type three-electrode cell. The working electrodes were the obtained thick-films. Both counter and reference electrodes were 1-mm-thick Li metal sheets (Rare Metallic, 99.90%). We used  $\text{LiClO}_4$  dissolved in propylene carbonate (PC;  $\text{C}_4\text{H}_6\text{O}_3$ , Kishida Chemical Co., Ltd.) at concentration of 1 M as the electrolyte. Constant current charge–discharge tests were performed using an electrochemical measurement system (HZ-3000 Hokuto Denko Co., Ltd.) under a constant current of 0.1 mA (*ca.* 1–2 C) at 303 K with the cutoff potentials set as 0.005 V vs.  $\text{Li/Li}^+$  for charge and 2.000 V vs.  $\text{Li/Li}^+$  for discharge. To avoid oxidation, the active material powder and the obtained electrodes were kept in dry Ar gas throughout all experiments.

### 3. RESULTS AND DISCUSSION

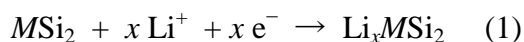
Figure 1(a) depicts charge–discharge curves of obtained thick-film electrodes of various metal silicides at the first cycles. For comparison, the figure also shows the curve of  $\text{LaSi}_2$  electrode which

has been previously reported [17]. The initial discharge (Li-extraction) capacities of  $\text{FeSi}_2$ ,  $\text{VSi}_2$ , and  $\text{MmSi}_2$  electrodes were about 30, 50, and 35  $\text{mA h g}^{-1}$ , respectively.



**Figure 1.** (a) Charge–discharge curves at the first cycles and (b) cycling performance of thick-film electrodes of various metal silicides,  $\text{FeSi}_2$ ,  $\text{VSi}_2$ ,  $\text{MmSi}_2$ . For comparison, the curve of  $\text{LaSi}_2$  electrode [17] was also shown.

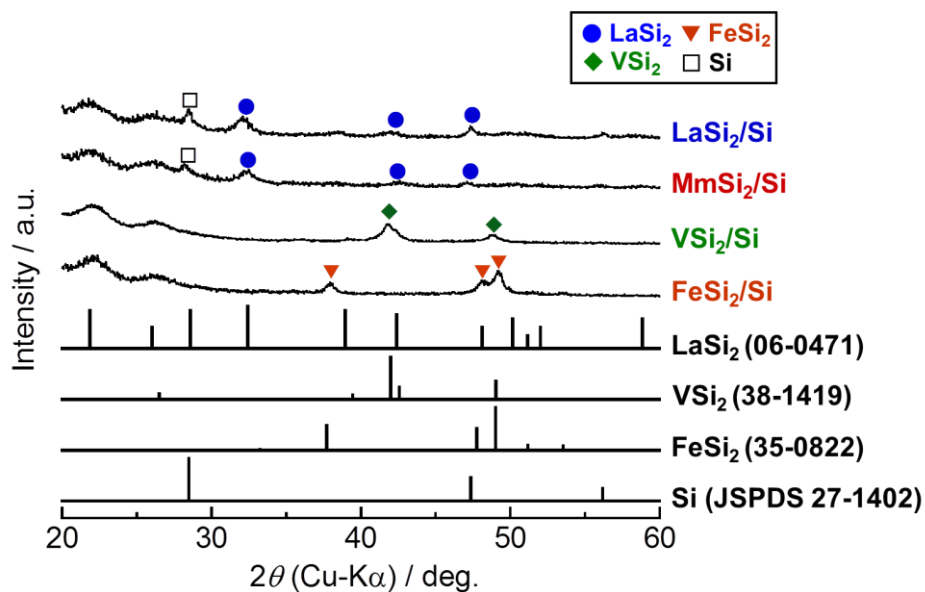
These values are comparable to the discharge capacity of the  $\text{LaSi}_2$  electrode ( $45 \text{ mA h g}^{-1}$ ), which is much lower than theoretical capacity of graphite anode ( $372 \text{ mA h g}^{-1}$ ). It was confirmed that the huge capacity of elemental Si is not manifested in these silicides because of their smaller storage amount of Li. Although the occupation site of Li in the crystal structure of these metal silicides ( $\text{MSi}_2$ ) in the alloying reaction has not been clearly found, we propose a following electrode reaction:



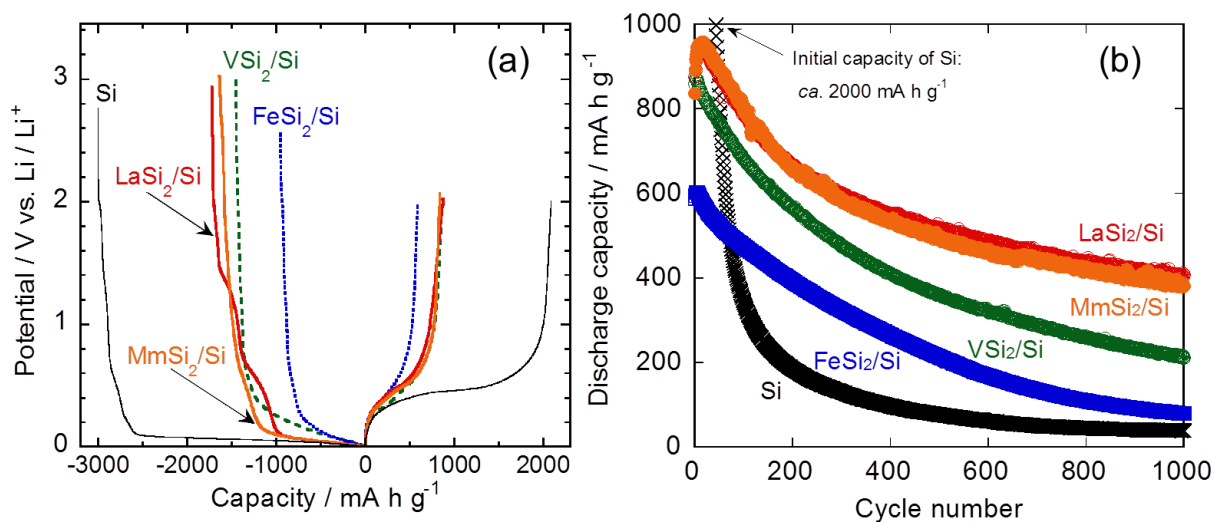
For these silicides, the maximum values of  $x$  were estimated to be 0.1–0.3. As a preliminary experiment by XRD for the  $\text{LaSi}_2$  electrode, no change in diffraction angle was found after Li-insertion with  $x = 0.3$ . Thus, Li ions are suggested to be stored at interstitial sites in the crystal structure of  $\text{LaSi}_2$  by the charge reaction. Figure 1(b) represents the changes in the discharge capacity of these metal silicide electrodes with respect to the cycle number. We consider that there is no significant difference in the discharge capacities of these electrodes because the difference is within only  $20 \text{ mA h g}^{-1}$ . In each case, very superb cycle stability was obtained for a period of 1000 cycles.

Figure 2 shows XRD patterns of composited active materials obtained by MA. Broad peaks were observed at 22 and 26 degrees, which are attributed to the polyimide films for oxidation resistant coating on the samples. For the composite powders of  $\text{LaSi}_2/\text{Si}$  and  $\text{MmSi}_2/\text{Si}$ , we can recognize XRD peaks of  $\text{LaSi}_2$  ( $\alpha\text{-ThSi}_2$  structure) in addition to a peak of Si. On the other hand, XRD peaks of only metal silicides appeared in cases of  $\text{VSi}_2/\text{Si}$  and  $\text{FeSi}_2/\text{Si}$ . However, the excess Si should be included in these composite powders obtained by MA. Thus, amorphous Si and/or less-crystalline Si must be

contained in the composite powder of  $\text{VSi}_2/\text{Si}$  and  $\text{FeSi}_2/\text{Si}$ . The longer milling time for  $\text{VSi}_2/\text{Si}$  and  $\text{FeSi}_2/\text{Si}$  probably causes lower crystallinity of Si in the powder. From these results, we confirmed that the composite active materials consisted of Si and metal silicides were successfully synthesized as expected.



**Figure 2.** XRD patterns of composite active materials consisted of Si and various metal silicides.



**Figure 3.** (a) Charge-discharge curves at the first cycles and (b) cycling performance of pristine Si electrode and composite electrodes consisted of  $\text{FeSi}_2/\text{Si}$ ,  $\text{VSi}_2/\text{Si}$ ,  $\text{MmSi}_2/\text{Si}$ . For comparison, the curve of  $\text{LaSi}_2/\text{Si}$  electrode [17] was also shown

Figure 3(a) displays the charge-discharge curves of the thick-film electrodes using the composite active materials consisting of Si and the silicides at the first cycles. For comparison, the

curves of pristine Si electrode and  $\text{LaSi}_2/\text{Si}$  composite electrode [17] are also showed in the figure. In every case, potential plateaus were observed at approximately 0.1 and 0.4 V vs.  $\text{Li}/\text{Li}^+$  in the charge and discharge reactions. These potential plateaus are attributed to the alloying and de-alloying reactions of Si with Li. It was thus obvious from the matching of the charge–discharge potentials that elemental Si in the composites acts as the active material which mainly contributes to insertion–extraction of Li ions. We notice that the thick-film electrodes of  $\text{VSi}_2/\text{Si}$  and  $\text{FeSi}_2/\text{Si}$  show inclined plateaus in the first charge curve. The inclined plateaus are possibly attributed to the lower crystallinity of Si in the composite active materials of  $\text{VSi}_2/\text{Si}$  and  $\text{FeSi}_2/\text{Si}$ . The initial discharge capacity of the  $\text{FeSi}_2/\text{Si}$  composite electrode was  $690 \text{ mA h g}^{-1}$ , which is lower than that of the  $\text{LaSi}_2/\text{Si}$  composite electrode ( $870 \text{ mA h g}^{-1}$ ). On the other hand, the initial capacities of the  $\text{VSi}_2/\text{Si}$  and  $\text{MmSi}_2/\text{Si}$  electrodes were 860 and  $840 \text{ mA h g}^{-1}$ , and these values are almost same as the capacity of the  $\text{LaSi}_2/\text{Si}$  electrode. Figure 3(b) presents the dependence of the discharge capacity on the cycle number for these electrodes. The pristine Si electrode showed rapid capacity decay until the 100th cycle, resulting in poor electrode performance. The rapid capacity decay is attributed to a collapse and an electrical isolation of Si induced by its significant volumetric change during the charge–discharge reactions. In contrast, the cycling stability was improved in the composite electrodes consisted of Si and metal silicides though their initial capacities were much lower than the capacity of the pristine Si electrode. It is notable that the  $\text{MmSi}_2/\text{Si}$  electrode exhibited excellent cycling performance equivalent to that of the  $\text{LaSi}_2/\text{Si}$  electrode, where its capacity of  $380 \text{ mA h g}^{-1}$  at the 1000th cycle exceeds the theoretical capacity of graphite anode practically used.

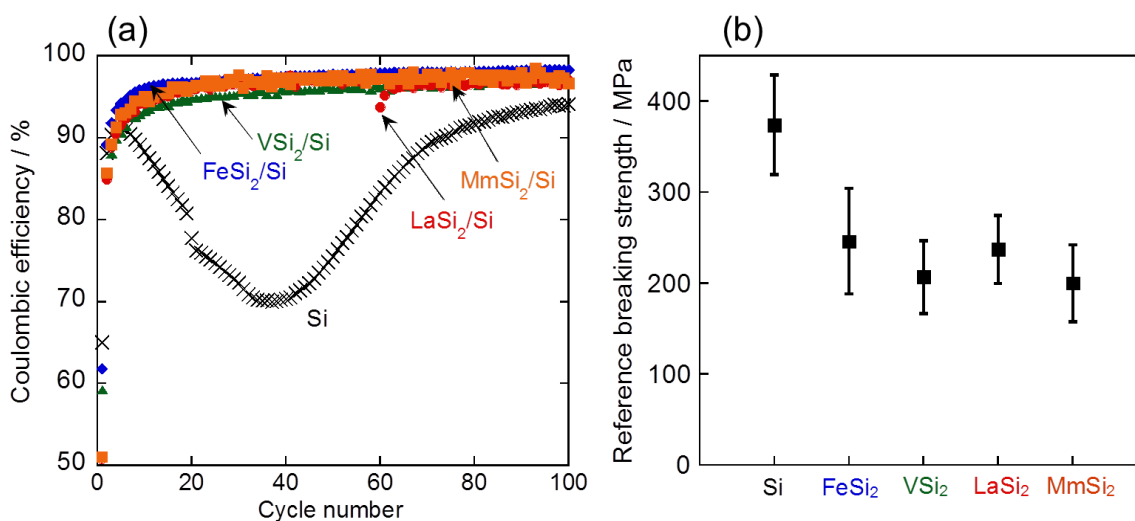


**Figure 4.** (a) Coulombic efficiencies of pristine Si electrode and composite electrodes consisted of various metal silicides. (b) Reference breaking strength of particles of Si,  $\text{FeSi}_2$ ,  $\text{VSi}_2$ ,  $\text{LaSi}_2$ , and  $\text{MmSi}_2$ .

Due to a lower cost of Mm in comparison with elemental La, the performance of the  $\text{MmSi}_2/\text{Si}$  electrode makes it more suitable for application as anodes in next-generation Li-ion battery. Figure

4(a) gives the coulombic efficiencies of the thick-film electrodes of the pristine Si and the metal silicide composites in the first 100 cycles. The declination of the coulombic efficiency indicates the physical detachment and the electrical isolation of the active material from the substrate of current collector. A significant declination was observed for the pristine Si electrode during the initial 40 cycles. We can clearly recognize that the declination was substantially suppressed in cases of the metal silicide composites.

The reason of improved cycling performance and higher coulombic efficiencies in the composite electrodes is presumably attributed to the electrical and mechanical properties of the silicide matrices in the electrodes. The electrical resistivity of pressed Si powder was  $1.6 \times 10^4 \Omega \text{ cm}$ , which was determined by the resistance measurement under the uniaxial pressure in this study. On the other hand, the metal silicides showed the electrical resistivity lower than  $6.5 \Omega \text{ cm}$ . These results revealed that the metal silicides have much better electrical conductivity in comparison with the pristine Si. Therefore, it is clear that the silicide matrices greatly improve the conductivity of the composite electrodes, and that the electrical isolation of Si can be effectively suppressed by the silicide matrices. The improved conductivities have been reported for other composite anode materials, Cu–Si/graphite [22] and  $\text{Co}_3\text{O}_4/\text{Al}$  [23].

Figure 4(b) compares the reference breaking strength measured for particles of the pristine Si and the metal silicides,  $\text{FeSi}_2$ ,  $\text{VSi}_2$ ,  $\text{LaSi}_2$ , and  $\text{MmSi}_2$ . The errors bars in the figure indicate the standard deviation of measured values. The reference breaking strength of the metal silicides is relatively smaller than that of the pristine Si, which suggests that the metal silicides are easily deformed by a lower pressure.

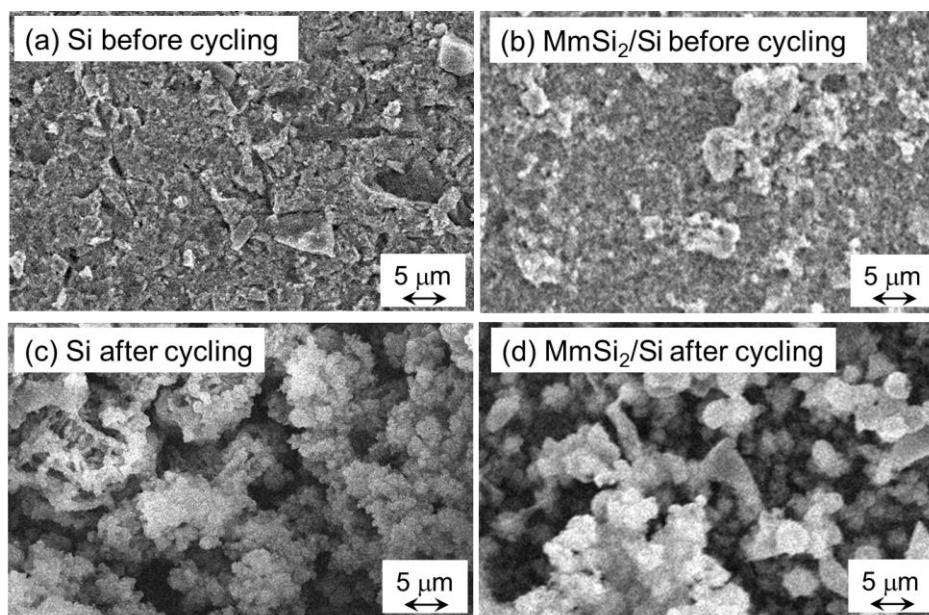


**Figure 5.** SEM images of thick-film electrodes of (a) pristine Si and (b)  $\text{MmSi}_2/\text{Si}$  composite before charge–discharge cycling tests, and (c) pristine Si and (d)  $\text{MmSi}_2/\text{Si}$  composite after charge–discharge cycling tests.

Consequently, it was confirmed that the metal silicides in the composite electrodes can act as a matrix which reduces the stress induced by the volumetric changes of Si. The Mm consists of four light-rare-earth elements (La, Ce, Pr, and Nd), and these elements have nearly identical chemical and physical properties. Thus, it is a reasonable result that the reference breaking strength of  $MmSi_2$  is as small as that of  $LaSi_2$ .

Figure 5 portrays SEM images of the thick-film electrodes of the pristine Si and the  $MmSi_2/Si$  composite before and after charge–discharge cycling tests. Before the cycling test, both electrodes of Si and  $MmSi_2/Si$  showed a flat surface. In contrast, a drastic change of the surface morphology, pulverization and generation of dense cracks, was observed for the pristine Si electrode after the cycling test as shown in Fig. 5(c). Similarly, the  $MmSi_2/Si$  electrode showed a collapse of surface structure as shown in Fig. 5(d). However, the size of the active material particles is larger than that of the pristine Si electrode after the cycling test, which implies that the pulverization of Si is partially suppressed by an existence of  $MmSi_2$  matrix in the composite electrode.

The difference in the cycling performance appears among the composite electrodes of  $FeSi_2/Si$ ,  $VSi_2/Si$ , and  $MmSi_2/Si$  though no remarkable difference was observed for the electrical resistivity and the reference braking strength in these electrodes. We are herewith proposing the enthalpy of solution, one of parameters indicating thermodynamic stability, for the metal silicides as the origin of the difference. Niessen and co-workers have reported the enthalpy of solution at infinite dilution for various compounds [24]. According to their study, the enthalpy of solution for Fe–Si, V–Si, and La–Si are  $-67$ ,  $-121$ , and  $-285$   $\text{kJ mol}^{-1}$ . These negative values indicate that these silicides are thermodynamically stable materials. Furthermore, it is suggested that these silicides are more stable with increasing the absolute value of these enthalpy. On the other hand, the enthalpy of solution for Si–Li has been reported to be  $-51$   $\text{kJ mol}^{-1}$  [24]. We should note that the absolute value of the enthalpy for Si–Li is smaller than that for these silicides. Thus, the metal silicides do not decompose, and can stably exist during the alloying/de-alloying reactions of Si with Li for a long period as following the equation (1). Therefore, the cycling performance of the composite electrode became better with increasing the absolute value of the enthalpy because the improvement of the electrical conductivity and the release of the stress are attributed to the silicide matrix which is thermodynamically more stable. As for the  $MmSi_2$  matrix, we consider that the  $MmSi_2/Si$  composite electrode exhibited excellent cycling performance because  $MmSi_2$  matrix is very stable similarly to  $LaSi_2$  matrix due to the nearly identical properties among La, Ce, Pr, and Nd.

#### 4. SUMMARY

We synthesized the composite active materials of Si and the metal silicides,  $FeSi_2/Si$ ,  $VSi_2/Si$ , or  $MmSi_2/Si$ , by the MA method, and prepared the thick-film electrodes using these composites by the GD method. The anode properties of these electrode were investigated. The  $MmSi_2/Si$  composite electrode exhibited superb cycling performance, the discharge capacity of  $380$   $\text{mA h g}^{-1}$  was maintained even at the 1000th cycle. The electrical resistivity and the reference breaking strength were measured for the active material powder of the metal silicides. We discussed the relationship between

the electrode performance and properties of these silicide matrices, the electrical resistivity, the referential breaking strength, and the thermodynamic stability. The excellent performance of the composite electrode is probably attributed to the thermodynamically stable  $MmSi_2$  matrix which improves the electrical conductivity of the composite electrode and releases the stress induced by the volumetric change of Si.

#### ACKNOWLEDGMENTS

This work was partially supported by a grant from the project, Development of High-performance Battery System for Next generation Vehicles (Li-EAD Project), from the New Energy and Industrial Technology Development Organization (NEDO) of Japan. This work was partly supported from the Grant-in-Aid for Scientific Research of Ministry of Education, Culture, Sports, Science and Technology (MEXT), Japan. The authors thank Dr. T. Iida for his kind assistance. The authors also gratefully acknowledge Mr. K. Kato for his assistance with electrical resistivity measurements.

#### References

1. J. O. Besenhard, J. Yang, M. Winter, *J. Power Sources*, 68 (1997) 87.
2. U. Kasavajjula, C. S. Wang, A. J. Appleby, *J. Power Sources*, 163 (2007) 1003.
3. N. Ding, J. Xu, Y. Yao, G. Wegner, I. Lieberwirth, C. Chena, *J. Power Sources*, 192 (2009) 644.
4. C. J. Wen, R. A. Huggins, *J. Solid State Chem.*, 37 (1981) 271.
5. W.-R. Liu, Z.-Z. Guo, W.-S. Young, D.-T. Shieh, H.-C. Wu, M.-H. Yang, Nae-Lih Wu, *J. Power Sources*, 140 (2005) 139.
6. H. S. Kim, K. Y. Chung, B. W. Cho, *J. Power Sources*, 189 (2009) 108.
7. B. A. Boukamp, G. C. Lesh, R. A. Huggins, *J. Electrochem. Soc.*, 128 (1981) 725.
8. V. A. Sethuraman, M. J. Chon, M. Shimshak, V. Srinivasan, P. R. Guduru, *J. Power Sources*, 195 (2010) 5062.
9. H. Sakaguchi, T. Toda, Y. Nagao, T. Esaka, *Electrochem. Solid-State Lett.*, 10 (2007) J146.
10. G. A. Roberts, E. J. Cairns, J. A. Reimer, *J. Power Sources*, 110 (2002) 424.
11. A. Netz, R. A. Huggins, W. Weppner, *J. Power Sources*, 119–121 (2003) 95.
12. J. Wolfenstine, *J. Power Sources*, 124 (2003) 241.
13. H.-Y. Lee, Y.-L. Kim, M.-K. Hong, S.-M. Lee, *J. Power Sources*, 141 (2005) 159.
14. Y.-L. Kim, H.-Y. Lee, S.-W. Jang, S.-H. Lim, S.-J. Lee, H.-K. Baik, Y.-S. Yoon, S.-M. Lee, *Electrochimica Acta*, 48 (2003) 2593.
15. S. Zhou, D. Wang, *ACS Nano*, 4 (2010) 7014.
16. T. Iida, T. Hirono, N. Shibamura, H. Sakaguchi, *Electrochemistry*, 76 (2008) 644.
17. H. Sakaguchi, T. Iida, M. Itoh, N. Shibamura, T. Hirono, *IOP Conf. Series: Mater. Sci. Eng.*, 1 (2009) 012030.
18. H. Usui, Y. Kashiwa, T. Iida, H. Sakaguchi, *J. Power Sources*, 195 (2010) 3649.
19. H. Usui, H. Nishinami, T. Iida, H. Sakaguchi, *Electrochemistry*, 78 (2010) 329.
20. H. Usui, M. Shibata, K. Nakai, H. Sakaguchi, *J. Power Sources*, 196 (2011) 2143.
21. H. Usui, Y. Yamamoto, K. Yoshiyama, T. Itoh, H. Sakaguchi, *J. Power Sources*, 196 (2011) 3911.
22. P. Wang, Y. NuLi, J. Yang, Y. Zheng, *Int. J. Electrochem. Sci.*, 1 (2006) 122.
23. X. Lei, J. Ma, Y. Sun, *Int. J. Electrochem. Sci.*, 6 (2011) 573.
24. A. K. Niessen, F. R. de Boer, R. Boom, P. F. de Châtel, W. C. M. Mattens, *Calphad*, 7 (1983) 51.